Future climate change: Implications for Indian summer monsoon and its variability

Murari Lal[†,*], T. Nozawa[#], S. Emori[#], H. Harasawa[#], K. Takahashi[#], M. Kimoto[‡], A. Abe-Ouchi[‡], T. Nakajima[‡], T. Takemura[‡] and A. Numaguti[**]

[†]Centre for Atmospheric Sciences, Indian Institute of Technology, New Delhi 110 016, India
[#]National Institute of Environmental Studies, Tsukuba, Japan
[‡]Center for Climate System Research, University of Tokyo, Japan
[**]Hokkaido University, Japan

The broad climatological features associated with the Asian monsoon circulation, including its mean state and intraseasonal and interannual variability over the Indian subcontinent, as simulated in the CCSR/NIES coupled A–O GCM in its control experiment are presented in this paper. The model reproduces the seasonal cycle as well as basic observed patterns of key climatic parameters, in spite of some limitations in simulation of the monsoon rainfall. While the seasonality in rainfall over the region is well simulated and the simulated area-averaged monsoon rainfall is only marginally higher than the observed rainfall, the peak rainfall is simulated to be about two-thirds of the observed precipitation intensity over central India.

The transient experiments performed with the model following the four SRES 'Marker' emission scenarios, which include revised trends for all the principal anthropogenic forcing agents for the future, suggest an annual mean area-averaged surface warming over the Indian subcontinent to range between 3.5 and 5.5°C over the region during 2080s. During winter, India may experience between 5 and 25% decline in rainfall. The decline in wintertime-rainfall over India is likely to be significant and may lead to droughts during the dry summer months. Only a 10 to 15% increase is projected in area-averaged summer monsoon rainfall over the Indian subcontinent. The date of onset of summer monsoon over India could become more variable in future.

CONSIDERABLE improvement in the simulation of present-day climate on regional scales has taken place in recent years[1]. There have also been refinements made in coupled global climate models to make them more self-deterministic, e.g. the use of self-determined cloud optical properties to replace the prescribed values[2] or the sensitivities of a coupled system to changes in cloud amount and albedo feedbacks have been explored[3]. The coupled atmosphere–ocean general circulation models (A–O GCMs) are now being used for studies related to the natural variability of the climate system and its response to changes in anthropogenic radiative forcings[4].

Simulation of the Asian monsoon circulation has proven to be a critical test of the ability of global climate models (GCMs) in simulating the tropical climate variability[5]. The numerical experiments performed with the state-of-the-art A–O GCMs are able to realistically simulate the planetary and regional-scale circulations associated with the Indian summer monsoon. These models simulate the large-scale climatological features in response to global forcings such as land–sea distribution, orography and differential heating reasonably well[6,7]. However, the simulation of seasonal rainfall as well as its spatial and temporal variability over the Indian subcontinent has remained rather poor in most GCMs, primarily due to coarse horizontal resolution which restricts the representation of the complexity of topography and coastlines, and the limitations in physical parameterization of sub-grid scale processes[8].

Regional characteristics, e.g. land–sea thermal contrast, orographic features, vegetation cover and inland water basins, play an important role in the establishment of summer monsoon over the Indian subcontinent. The thermal structure of the adjoining oceanic areas – the Arabian Sea, the Bay of Bengal and the South Indian Ocean and its temporal variations, also have a modulating influence on the monsoon. Significant interannual and intraseasonal variabilities in the observed monsoon rainfall are displayed over this region, resulting in recurrent droughts and floods. In India, drought risk may represent potentially the most serious impact of climate change. In this respect, the future projections of changes in monsoon rainfall variability over the Indian subcontinent are very crucial.

We examine here the skill of the Japanese Centre for Climate System Research/National Institute for Environmental Studies (CCSR/NIES) A–O GCM in simulating the annual cycle of observed climatological features associated with the Asian monsoon circulation, in the control simulation for the current climate forcing conditions. A comparison of the observed and simulated broad-scale patterns of mean sea level pressure, surface air temperature

*For correspondence. (e-mail: mlal@cas.iitd.ernet.in)

and precipitation over the Indian subcontinent is made. The onset and advancement of monsoonal activity and temporal rainfall variations, as simulated by the model during the summer monsoon season over India, are assessed. We also project the likely future changes in climatology of the Indian subcontinent and in the intraseasonal and interannual variability of the summer monsoon, as simulated by the CCSR/NIES A–O GCM, under the anthropogenic radiative forcings determined from future emission scenarios in this paper.

The IPCC Special Report on emission scenarios (SRES) recently proposed a new set of scenarios which covers a wide range of the main demographic, technological and economic driving forces of future emissions[9]. Four 'Marker' scenarios (namely A1, A2, B1 and B2) have been identified, each of which describes a different world evolving through the 21st century and each of which may lead to quite different greenhouse gas emission trajectories. The scenario B1 projects the most conservative future emission of greenhouse gases, while A2 is characteristic of scenarios with higher rates of greenhouse gas emissions in combination with higher sulphur and other aerosol emissions. The A1 scenario family has been further divided into three groups that describe alternative directions of technological change in the energy system. The three A1 groups are distinguished by their technological emphasis: fossil-intensive (A1FI), non-fossil energy sources (A1T), or a balance across all sources (A1B)[10]. The future projections of aerosol loading as envisaged in SRES 'Marker' scenarios are significantly lower compared to IS92a scenario (Figure 1). The SRES scenarios exclude the effects of climate change and climate policies on society and the economy (non-intervention). The new emission scenarios suggest that the global mean surface temperature could increase by between 1.4 and 3°C for low emission scenarios and between 2.5 and 5.8°C for high emission scenarios by 2100 with respect to 1990. Globally averaged precipitation is projected to increase, but at the regional scale both increases and decreases are projected. These projections are considered more realistic than the IS92a emission scenario used earlier in transient experiments with A–O GCMs. In this respect, the projections of regional climate change reported in this paper are an update on those published earlier[11] and should provide more meaningful applications in vulnerability assessment.

The CCSR/NIES A–O GCM

The atmospheric component of this model has been developed at CCSR of the University of Tokyo and NIES in Japan. The basic equations include three-dimensional primitive equations and the prognostic variables are horizontal velocity, temperature, surface pressure, specific humidity, cloud liquid water, soil temperature, soil moisture and snow depth[12]. The horizontal discretization is done following spectral transformation method with Gaussian grid at T21 resolution. The vertical discretization follows terrain-following coordinate with 20 levels. The model integration is done following leap-frog scheme with a time step of about 40 min. The physical processes include two-stream k-distribution radiative transfer scheme[13]. Cumulus convection is treated through simplified Arakawa–Schubert parameterization scheme. Cloud liquid water is estimated following prognostics of the total water content based on Le Treut and Li[14] approach. The treatment of boundary layer turbulence follows the Mellor–Yamada level-2 turbulence scheme, while the surface fluxes are calculated following the bulk scheme of Louis[15]. The land surface processes include multi-layer treatment for heat conduction and a bucket model for hydrology. The gravity wave drag due to orography is treated following McFarlane[16] scheme.

In addition to individual treatment of the primary greenhouse gases, namely CO_2, CH_4, N_2O and stratospheric and tropospheric O_3 including their scenario-dependent temporal variations, thirteen species of CFCs are also treated in the model. The model considers four aerosol species, namely sulphate, carbon, dust and sea salt. While dust and sea salt aerosols are supplied as climatology with seasonal variations, the carbonaceous and sulphate aerosols follow the SRES 'Marker' scenarios. The aerosol concentrations are calculated off-line by an aerosol transport model of Takemura *et al.*[17]. The aerosol scattering is explicitly represented to account for their direct effects. The indirect effects of aerosol on effective radius of cloud droplet and on precipitation efficiency are treated through a relationship between cloud droplet and aerosol number concentrations.

The ocean model has been developed by Yamanaka and Tajika[18] to predict currents, potential temperature and salinity and has numerical scheme similar to the Geophysical Fluid Dynamics Laboratory (GFDL)'s Bryan Cox model, except that the weighted upcurrent scheme is introduced to the advection terms in the temperature and salinity equations[19]. The boundary conditions include rigid lid surface with nonslip condition and zero normal fluxes of heat and salinity at the lateral boundaries. The horizontal discretization is done at 2.8° × 2.8° latitude/ longitude and the model has 17 unequally spaced vertical levels with realistic bottom topography; the uppermost layer is 50 m and no mixed layer model is introduced. The sea-ice component of the model is based on Semtner[20] and calculates snowfall, sublimation, surface melt and bottom melt or freeze. A river-routing model is also included with 50 river mouths, following Miller *et al.*[21]. In coupled mode, flux adjustment for heat and water is applied to overcome drift in long time integration. For further details on coupling procedures and experimental design, the reader is referred to Abe-Ouchi[22] and Emori *et al.*[23].

The study region and data used

The geographic region of interest in this study is the summer monsoon area bounded by latitudes 5°N to 35°N and longitude 65°E to 110°E (Indian subcontinent and adjoining seas). The simulated climatology is constructed by averaging over a 30-year period (1961–90) representative of the present-day climate in the control reference experiment. For all validation purposes, we have analysed the data for northern hemisphere winter (December, January and February: DJF) and summer monsoon season (June, July, August and September: JJAS) in addition to the annual means. The observed climatology for mean sea-level pressure used in this study is based on the average of 23 years' data (1973–95 period) from National Center for Environmental Prediction and National Center for Atmospheric Research (NCEP/NCAR) re-analyses[24]. The observed surface air temperature and precipitation climatology used here are those of Legates and Willmott[25] and New *et al.*[26]. The observed surface air temperature and precipitation climatology are likely to be less realistic in and around the mountainous regions and over the oceans due to sparsity of observations.

Daily data for rainfall simulated by the model have also been analysed for the period from 1 May until 30 October during each of the 30-year (1961–90) period to explore the intraseasonal and interannual variability in Indian summer monsoon rainfall over Central India (land points only confined to latitudes 18°N to 30°N and longitudes 67°E to 90°E). The observed daily rainfall data used for comparison are the average of 10 selected stations (Akola, Barrackpore, Bhubaneshwar, Gwalior, Indore, Jabalpur,

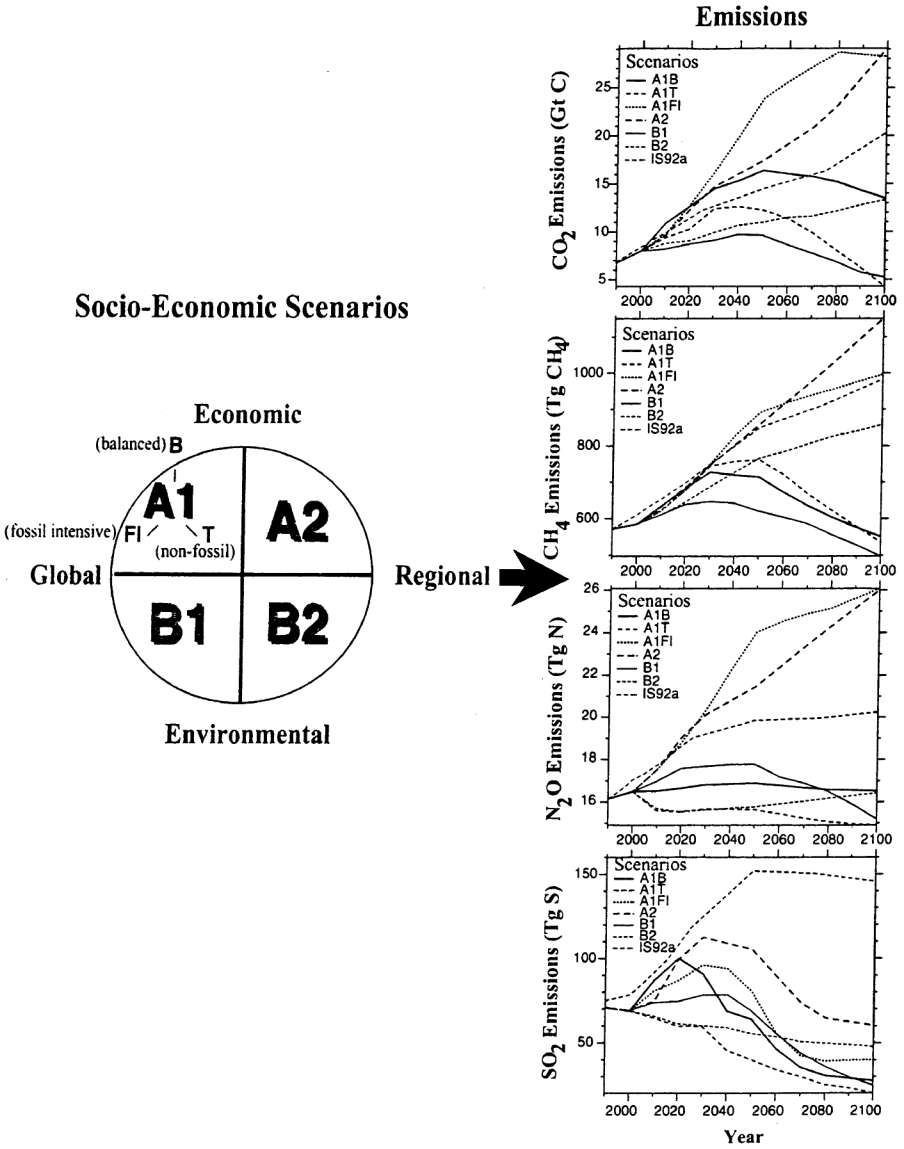

Figure 1. Comparison of future trends in emission of greenhouse gases and sulphur dioxide under IS92a and new SRES 'Marker' scenarios.

Powerkheda, Raipur, Ranchi and Udaipur) for each of the 25-year (1966–90) period. These stations are evenly distributed over space and have been selected such that they represent the daily rainfall characteristics of broad region covering the central plains of India. For future projections of change in key climatic elements, we have used the data generated in the transient experiments over three 30-year periods centred around 2020s, 2050s and 2080s.

Next, we shall present the skill of the CCSR/NIES A–O GCM in simulating the annual and seasonal mean climatology over the Indian subcontinent. Much of our emphasis in model validation is restricted only to surface parameters, as these are of direct relevance to impact assessment studies. The onset of the summer monsoon over the Indian subcontinent as inferred from the area-averaged daily rainfall time series will also be discussed.

Comparison of model simulation with observed climatology

The CCSR/NIES A–O GCM has been able to simulate important aspects of the large-scale northern and southern hemispheric climatology reasonably well, as confirmed by verification with NCEP re-analyses. The monsoon is, in general, considered as a manifestation of the seasonal migration of the planetary scale equatorial trough or tropical convergence zone (TCZ). The simulated seasonal migration of TCZ in the monsoon regions of the Africa–Asia sector is close to the climatological circulation features. The location and strength of upper air westerly jet over the northern Indian subcontinent during winter and the tropical easterly jet during monsoon season are also found to be in fair agreement with observed climatology. In view of this, we shall focus here only on the surface climatology of the Indian subcontinent.

Mean sea level pressure

The annual cycle of the mean sea level (MSL) pressure has the largest amplitude over the Asian continent. Over the Indian subcontinent, the MSL pressure distribution is characterized by high pressure over land and low pressure over the adjoining Indian Ocean during winter and the reverse during summer monsoon season. The simulated MSL pressure distribution pattern has some correspondence to the observed pattern both during January and July, the representative months for winter and monsoon, except over the Himalayan region. The seasonal heat low

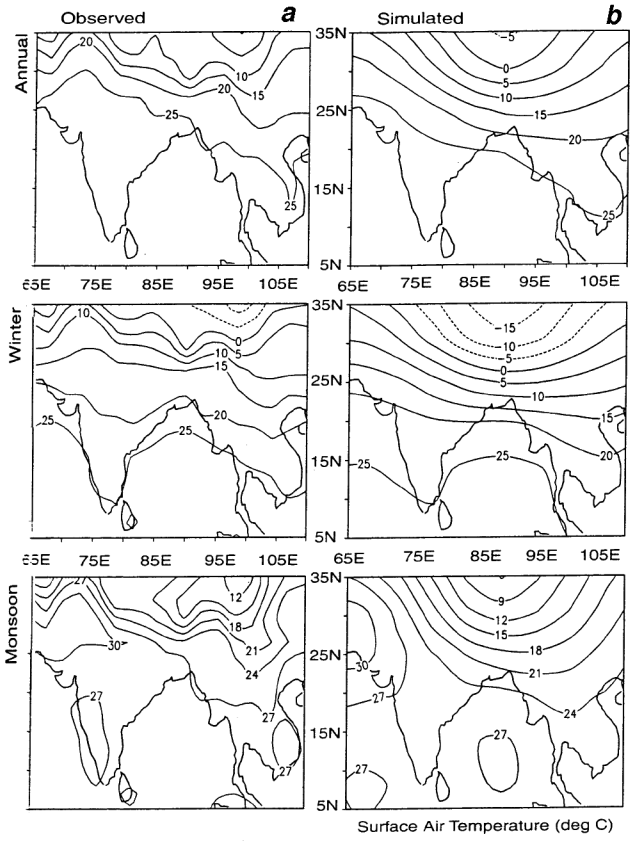

Figure 2. Spatial distribution of annual and seasonal mean surface air temperatures (°C) over Indian subcontinent as (*a*) observed and (*b*) simulated by the model.

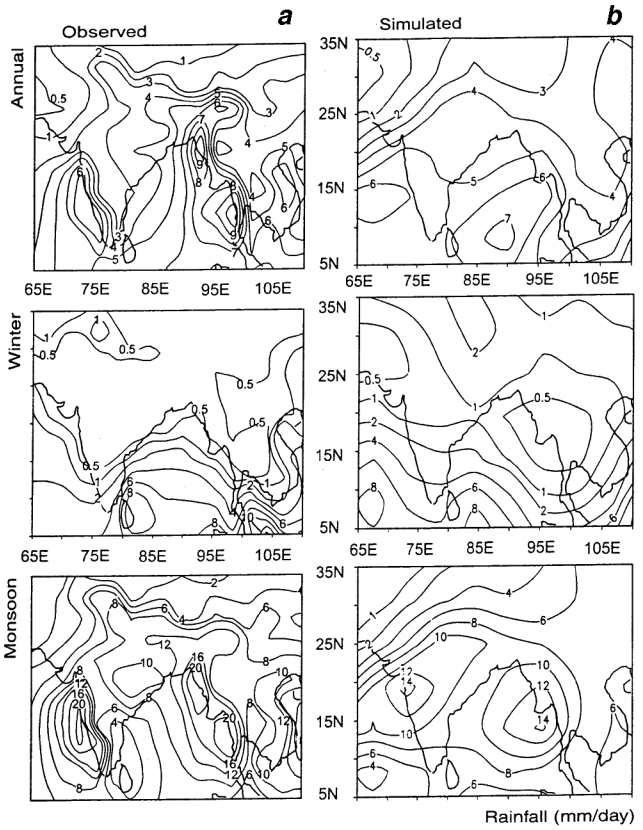

Figure 3. Spatial distribution of annual and seasonal mean rainfall (mm/day) over Indian subcontinent as (*a*) observed and (*b*) simulated by the model.

simulated by the model over north-west India in July is, however, rather deep compared to observed climatology. The orientation of the monsoon trough along the Indo-Gangetic plains is also rather poorly simulated.

With a view to quantitatively assessing the skill in model simulation, we have computed spatial pattern correlation coefficients (SPCC – a measure of similarity of the pattern structure over the region) and root mean square errors (RMSE – a measure of the absolute error between the two fields) between the simulated and the observed MSL pressure for January and July. The approach for calculating the SPCC and RMSE is similar to that described in Wigley and Santer[27]. The calculations involve interpolation of the model-simulated and observed data to a common grid configuration of T-42 resolution using a third-order polynomial interpolation scheme (it produces minimal modification of the original field). The SPCCs between the simulated and the observed MSL pressure in the region bounded by 5°N–30°N and 65°E–105°E (note that Tibetan Plateau has been excluded for SPCC and RMSE calculations, as the observed climatology for region is questionable and the model simulations are believed to be poor due to unresolved orographic features) are estimated to be 0.69 and 0.73 for January and July months, respectively. The RMSEs are considerably higher in January (4.7 hPa) relative to that in July (3.1 hPa).

As in observed climatology, the simulated surface winds across the equator over the Indian Ocean are south-easterlies and become south-westerlies over the Arabian Sea, peninsular India and the Bay of Bengal during the monsoon season. The model is able to reproduce the seasonal reversal in surface winds over the Indian subcontinent. The simulated trade winds are marginally stronger than those observed in the equatorial Indian Ocean. The cross-equatorial flow in simulated surface wind patterns during summer has an easterly bias along the eastern sector of the Indian Ocean. The 850 hPa winds over the land are somewhat stronger than those observed over the region. In general, the broad-scale features of the monsoon circulation have been captured by the model reasonably well.

Surface air temperature

The spatial distributions of observed and simulated surface air temperatures on an annual mean basis and during winter and monsoon are depicted in Figure 2. The simulated surface air temperature distribution is in fair agreement with observed climatology during both the seasons. The seasonal reversal in north to south thermal gradient over the Indian subcontinent is reasonably

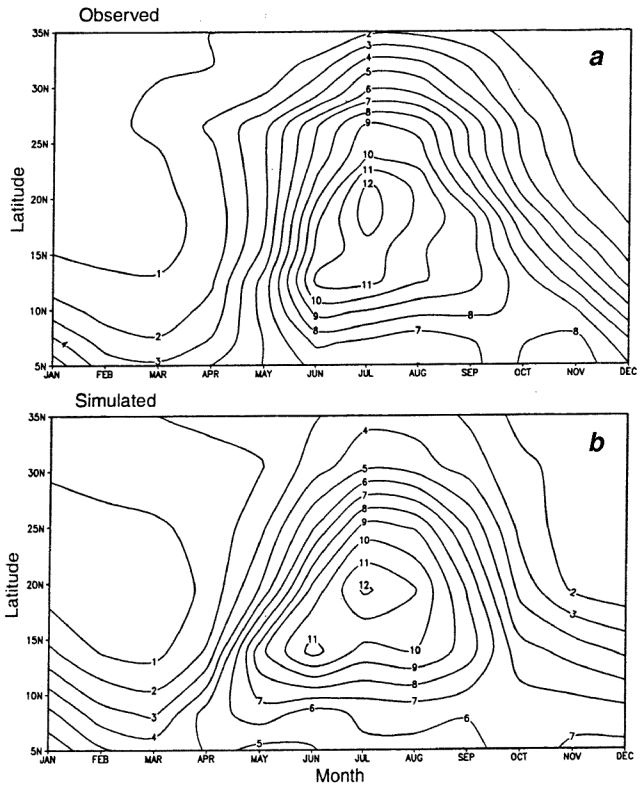

Figure 4. Temporal variation of (*a*) observed and (*b*) model-simulated present-day monthly zonal mean rainfall (mm/day) over Indian subcontinent (averaged over 65°E

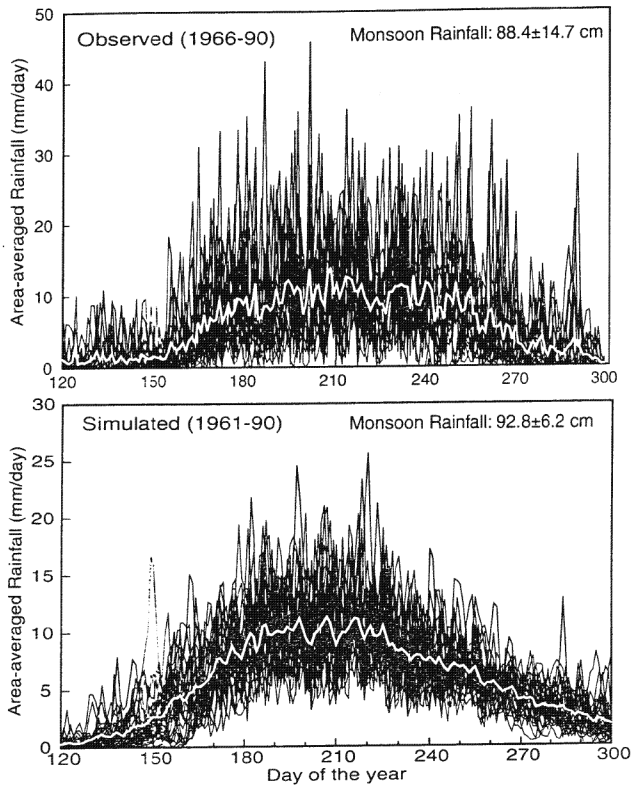

Figure 5. Comparison of present-day observed and model-simulated daily rainfall climatology during May to October over central India (1 June to 30 September cumulative rainfall and its standard deviation is given at the top right corner of the panel).

simulated by the model. The spatial range of surface temperature over India (~ 10.8°C) simulated by the model during July is, however, somewhat higher than that recorded (~ 9.4°C) in the observed climatology. The hottest region is the western margins of India, where the observed mean temperatures of 35°C in July are reproduced by the model. The SPCCs between the simulated and the observed surface temperatures are estimated to be 0.73 and 0.79 for winter and monsoon seasons, respectively. The RMSEs are low, both in winter (1.3°C) and during

The land to sea temperature gradient during the monsoon is regarded as the main driving force behind the monsoon circulation over the Indian subcontinent[28]. With a view to examining this aspect in the CCSR/NIES model simulation, we have computed seasonal mean surface temperatures over north-west India, where the observed heat low dominates during the monsoon season and over the east Arabian Sea (not shown in Figure 2, for brevity), where the monsoon winds become south-westerlies. The difference in simulated surface temperature between the two selected regions during monsoon season is 1.9°C as against the observed temperature difference of 2.1°C. Thus, the model is able to produce the observed thermal force at the surface to drive the summer monsoon circulation. This suggests that the CCSR/NIES model has a moderate skill in reproducing the observed seasonal surface temperature patterns over the Indian subcontinent.

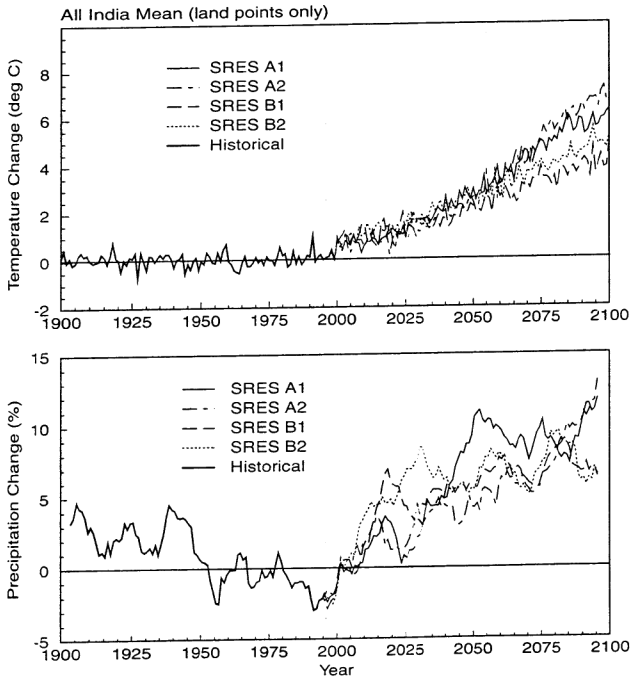

Figure 6. Trends in annual mean area-averaged temperature change (with respect to 1961–90 period) and rainfall change (in%, 10-year running mean) over the land regions of Indian subcontinent as simulated by the model under the four SRES 'Marker' forcing scenarios.

Precipitation

About 75 to 90% of the total annual rainfall over India occurs during the summer monsoon season. During winter, there is some rain over the northern parts of India (associated with western disturbances) and over the southern peninsular India (associated with north-east monsoon). The model is able to simulate the seasonality in rainfall as observed over the Indian subcontinent. The spatial pattern in observed mean monsoon precipitation is, however, fairly complex. The heaviest rains occur over the hilly states in the north-east and along the mountainous west coast (the Western Ghats and the Konkan coast). In addition to the primary monsoon rainbelt over the Indian subcontinent, significant rainfall occurs over the foothills of the Himalayas. There are no major deviations in the simulated rainfall relative to observed patterns during both the winter and monsoon seasons (Figure 3). The model, however, does not realistically simulate the orographic rainfall pattern near the Himalayan foothills and along the Western Ghats. The rainfall maxima along the west coast during monsoon season have a northward shift in the simulated pattern. The sharp gradient in

Table 1. Climate change projections* for Indian subcontinent under the four SRES emission scenarios

		Temperature change (°C)				Rainfall change (%)			
	Scenario	A1	A2	B1	B2	A1	A2	B1	B2
2020s	Annual	1.18	1.00	1.32	1.41	2.29	2.16	4.15	5.97
	Winter	1.19	1.08	1.37	1.54	0.39	– 1.95	4.36	3.64
	Monsoon	1.04	0.87	1.12	1.17	1.81	2.37	3.83	5.10
2050s	Annual	2.87	2.63	2.23	2.73	9.34	5.36	6.86	7.18
	Winter	3.18	2.83	2.54	3.00	3.22	– 9.22	3.82	3.29
	Monsoon	2.37	2.23	1.81	2.25	10.52	7.18	7.20	8.03
2080s	Annual	5.09	5.55	3.53	4.16	9.90	9.07	7.48	7.62
	Winter	5.88	6.31	4.14	4.78	– 19.97	– 24.83	– 4.50	– 10.36
	Monsoon	4.23	4.62	2.91	3.47	14.96	15.18	11.12	10.10

*Based on CCSR/NIES model experiments; Area-averaged for land regions only.

observed monsoon rainfall from west to east coast of peninsular India is also rather poorly simulated by the model. As regards seasonal variation of the observed and simulated monthly mean precipitation over the region, both the observed and model-simulated rainfall maxima during July–August are located at about 20°N (Figure 4). The northward advancement of simulated monsoon rains with the progression of the season is found to be realistic. Thus, it is obvious that, the continental TCZ is dominant over the Indian subcontinent, both in the observed climatology and in the model simulation.

Understanding the mechanisms of climate variability on a time scale of months to several years is a prerequisite for any prediction of climate. The Indian summer monsoon has linkages to not only global climate, but also regional energetics and its own inherent dynamics. To examine the progression of monsoonal currents and associated rainfall over the Indian subcontinent as well as its interannual and intraseasonal variability, we have analysed daily rainfall data for the 30-year period of control experiment performed with the CCSR/NIES A–O GCM. We shall now discuss our findings on this aspect.

Interannual and intraseasonal variability in monsoon rainfall

The Asian summer monsoon is one of most robust components of the global circulation system. From a global perspective, the Asian monsoon makes the largest contribution to the annual cycle of atmospheric heating which has significant impact on the planetary scale circulation[29]. It also makes a substantial contribution to the interannual variability of the tropospheric circulation. The centre of the highest interannual variability of kinetic energy is located in the Asian monsoon region[30]. The complex nature of the annual cycle of heating in the Indian-Pacific region makes the onset of the Indian summer monsoon quite abrupt and there are large intraseasonal variations between active and weak spells of monsoon rainfall. Significant periodicities have been identified in the long time series of observed Indian monsoon rainfall data[31]. Active spells of the Indian summer monsoon are associated with an intense intertropical convergence zone across the monsoon regime over the heated subcontinent. A dominant 30–60 day oscillation is discernible in circulation parameters and cloudiness over the region[32]. The ability of the CCSR/ NIES model in simulating some of these observed features of intraseasonal and interannual variability in the Indian monsoon circulation is examined here with a view to improving our understanding of the magnitude of regional warming as well as the likely changes in intraseasonal and interannual variability in response to future changes in anthropogenic radiative forcings.

The simulated daily rainfall data from 1 May to 30 October (183 days) during each of the 30-year period corresponding to the present-day climate have been analysed to explore the intraseasonal and interannual variability in Indian summer monsoon over central India (land points only confined to latitudes 18°N and 30°N and longitudes 67°E to 90°E). Figure 5 depicts the temporal variation of observed (1966–90) as well as simulated (1961–90) daily values of total rainfall averaged over central India from 1 May to 30 October for each year,

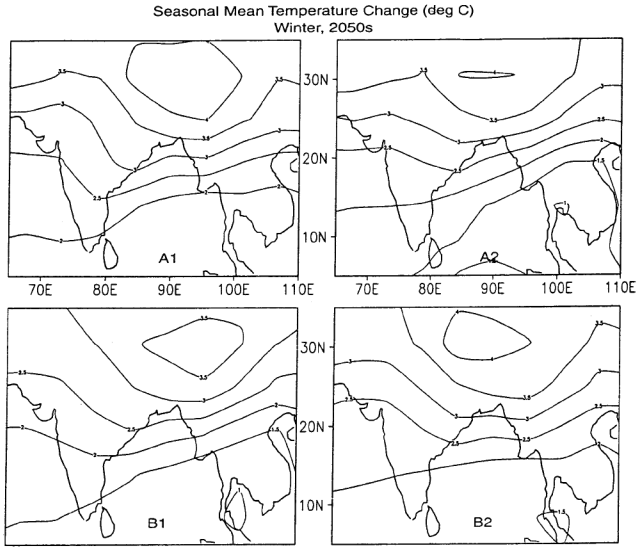

Figure 7. Spatial distribution of simulated surface air temperature change (°C) during winter season over Indian subcontinent in 2050s with respect to present-day under the four SRES 'Marker' forcing scenarios.

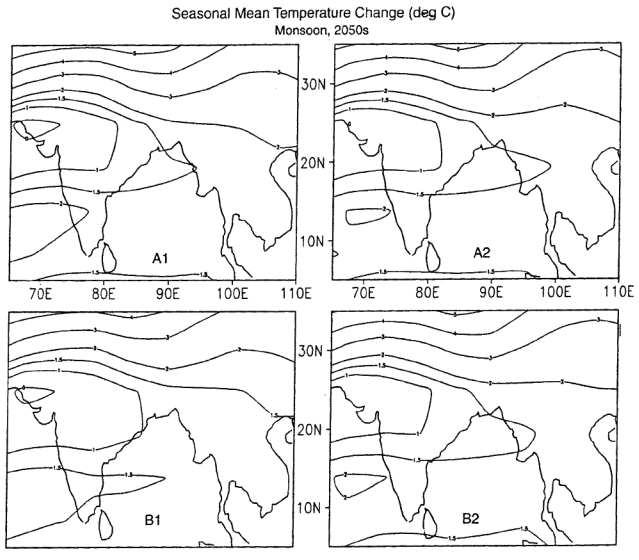

Figure 8. Spatial distribution of simulated surface air temperature change (°C) during monsoon season over Indian subcontinent in 2050s with respect to present-day under the four SRES 'Marker' forcing scenarios.

along with daily mean for the selected period (thick line). The rainfall maxima coincides with the peak monsoon activity over the region around mid-July. The seasonal total of simulated daily rainfall is marginally higher (by 4.9%) compared to observed rainfall, while the intensity of simulated daily rainfall is only two-thirds of that observed over the central plains of India. This could be attributed to far more number of rainy days in the model simulation as against observations. The year-to-year variability in monsoon rainfall simulated by the model (as inferred from the standard deviation of area-averaged monsoon rainfall for the 30-year period) is also significantly low (only 42% of the observed) relative to observed rainfall variability.

A large part of the intraseasonal variability in monsoon rainfall is associated with the various scales of monsoon circulation. It is thus pertinent to ascertain that the dominant scales are resolved appropriately in control experiment of the CCSR/NIES A–O GCM. During the monsoon season, an elongated zone of low pressure called the monsoon trough is a persistent feature over the Indian region, with its axis located at about 22°N in the east to about 27°N in the west. The low pressure systems forming over the Bay of Bengal during monsoon and moving inland along this monsoon trough are accompanied by moist convective clouds and cause intense spells of rainfall over the land regions of central India. The frequency and intensity of these synoptic scale systems in a particular year largely determine whether the monsoon rainfall has been excess, normal or deficient. It is, however, not possible to resolve these synoptic scale systems in global climate models with rather coarse horizontal resolution. An alternative approach towards identifying these synoptic scale disturbances in daily rainfall data is through identification of significant short-period oscillations in rainfall through mathematical tools, such as power spectrum analysis.

The detrended time series of simulated daily rainfall for the monsoon season (starting from 1 June to 30 September) averaged over central India has been analysed in frequency domain to estimate the raw spectral energies. The spectral energy computational procedure is similar to that adopted by Krishnamurti and Bhalme[33]. After smoothing with a 3-term weighted average by the Hanning method, the final spectral estimates are calculated from the raw spectral estimates. The analysis is repeated for each of the 30 consecutive years of control simulation (25-year period in case of observed daily rainfall) and then the averaged spectral energies for the selected period are calculated. The significance of the peaks is tested by fitting a curve at 90% level of confidence calculated by chi-square distribution. For central India, the simulated daily rainfall exhibits statistically significant spectral peaks at periodicities of about 13 and 10 days, in addition to short-term transients. These periodicities are not significantly different from those of 12 and 9 days obtained in observed rainfall time series. Observations[34] reveal that a large number of depressions within the monsoon trough form over the north Bay of Bengal in the time interval of 3 to 15 days. Therefore, the oscillations of time scales of about 7 to 13 days are likely to be associated with the synoptic scale disturbances themselves. The quasi-biweekly cycle with a oscillation of 13 days simulated in CCSR/NIES A–O GCM suggests that perhaps an average of 9 lows/depressions develop in the Bay of Bengal during a monsoon season and move across the central plains of India, which is close to the number frequency of 9.6 obtained in long-term climatology.

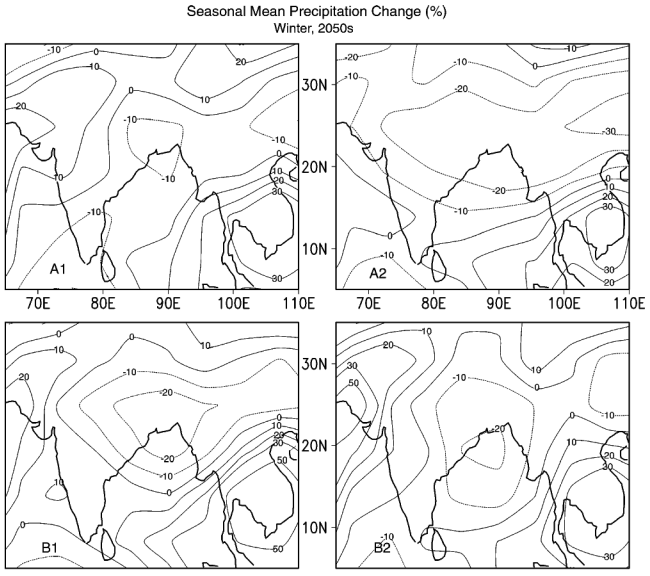

Figure 9. Spatial distribution of simulated winter-time rainfall change (in%) over Indian subcontinent in 2050s with respect to present-day under the four SRES 'Marker' forcing scenarios.

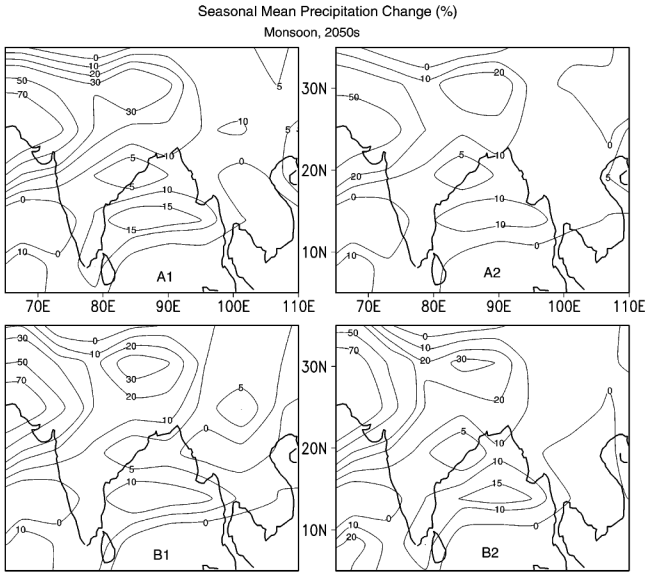

Figure 10. Spatial distribution of simulated monsoon rainfall change (in%) over Indian subcontinent in 2050s with respect to present-day under the four SRES 'Marker' forcing scenarios.

From the above, it is evident that the CCSR/NIES A–O GCM has some skill in simulating the south to north progression of monsoon. The model is able to resolve various scales of summer monsoon circulation and simulate a few observed characteristic features of the intraseasonal variability over the Indian subcontinent. The periodicities in simulated monsoon rainfall are comparable with the observations over the central Indian region. The model has, however, only limited ability in simulating the observed intraseasonal and interannual variabilities in the monsoon rainfall. Next, we present a brief account of the likely changes in monsoon climate and its variability as simulated by the CCSR/NIES model in its perturbed radiative forcing experiments.

Scenarios of future changes in climate and its variability

We shall focus here on the plausible climate change scenario for the Indian subcontinent as inferred from simulation experiments with enhanced greenhouse gas forcings. The precise magnitude of future changes in the mean and/or variance of climatological parameters on regional scales due to anthropogenic increases in greenhouse gases, is required to evaluate the vulnerability of the region to such changes. The key elements examined here are surface air temperature and precipitation. There are some additional elements also considered depending upon their importance in specific aspects of variability/change in the study region.

Over land regions of the Indian subcontinent, the area-averaged annual mean surface temperature rise by the end of this century is projected to be least in B1 scenario and maximum in A2 scenario and will range between 3.5 and 5.5°C (Figure 6). During winter, the area-averaged surface temperature increase over India by 2080s would be at least 4°C, while during monsoon, it may range between 2.9 and 4.6°C (Table 1). The projected surface warming is more pronounced during winter than during monsoon season. The warming during monsoon may produce an increase in water vapour and cloud water content which should not only enhance the reflectivity of the clouds (a negative feedback), but also contribute to an increase in the long-wave emissivity of cloud (a positive feedback, especially for the high cloud).

The spatial distribution of annual mean surface warming over the Indian subcontinent by 2050s, as a consequence of increase in anthropogenic radiative forcings (with respect to 1961–90) as simulated by the CCSR/NIES A–O

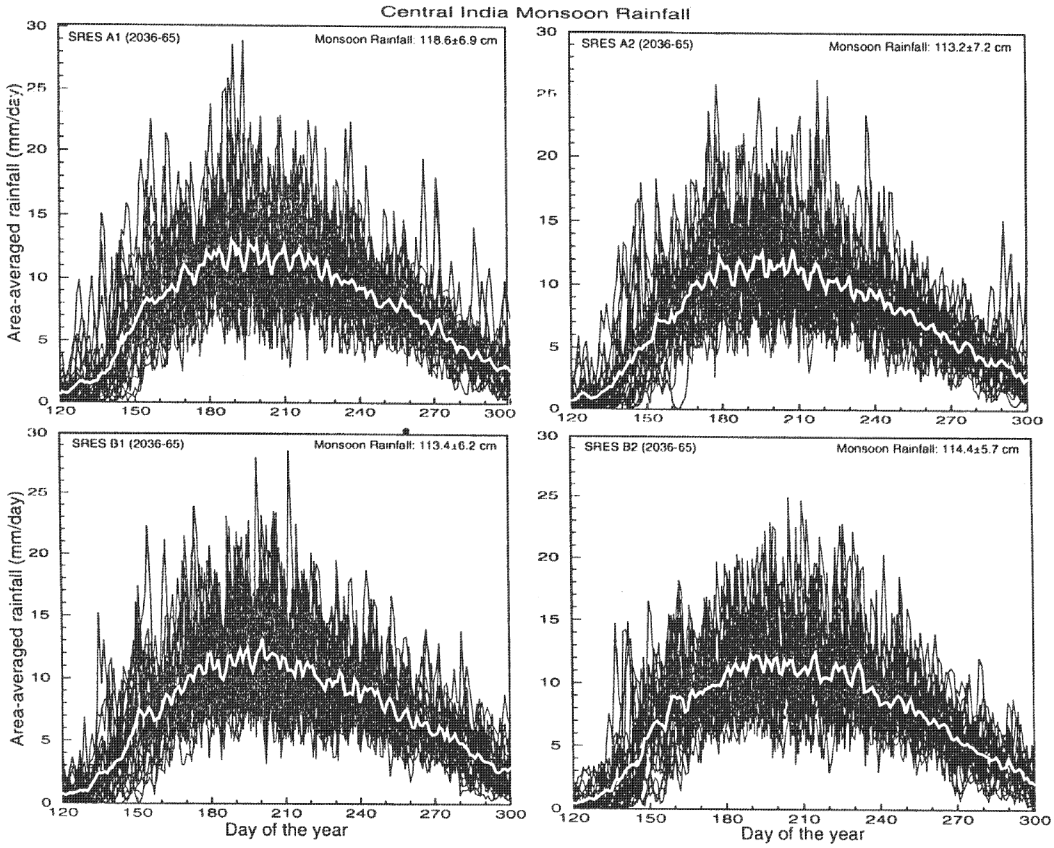

Figure 11. Model-simulated daily rainfall during May to October period over the central India for 30 years centered around 2050 (white line is the 30 year mean) under the four SRES 'Marker' forcing scenarios (1 June to 30 September cumulative rainfall and its standard deviation is given at the top right corner of the panels).

GCM, suggests that north India may experience an annual mean surface warming of 3°C or more, depending upon the future trajectory of anthropogenic forcings. The spatial pattern of temperature change has a large seasonal dependency. The model simulates peak warming of about 3°C over north and central India in winter (Figure 7). Over much of the southern peninsula, the warming is under 2°C during the winter season. During monsoon, temperature rise over south India is less than 1.5°C (Figure 8). The increase in surface temperature is more pronounced over north and east India (~ 2°C) during the monsoon season.

An increase of about 7 to 10% in area-averaged annual mean precipitation is simulated by the model over the Indian subcontinent by 2080s (Table 1). A decline of between 5 and 25% in area-averaged winter precipitation is likely. During the monsoon season, an increase in area-averaged summer precipitation of about 10 to 15% over the land regions is projected. The larger increase in surface temperature over land results in the intensification of heat low over north-west India and increased land–sea pressure gradient which strengthens the summer monsoon flow. The enhanced moisture convergence associated with stronger monsoon flow over the region in a warmer atmosphere results in increase in summer monsoon precipitation.

Contrary to previous projections[11], the new simulation experiments suggest appreciable change in spatial pattern of winter as well as summer monsoon precipitation over land regions of the Indian subcontinent. This could be attributed to inclusion of more realistic estimates of regional aerosol concentrations as well as the indirect radiative forcing due to aerosols. A decrease of between 10 and 20% in winter precipitation over most parts of central India is simulated for 2050s (Figure 9). During monsoon season, the results suggest an increase of 30% or more in precipitation over north-west India by 2050s (Figure 10). The western semi-arid margins of India could receive higher than normal rainfall in a warmer atmosphere.

In order to examine the likely changes in intraseasonal and interannual variability in summer monsoon over the Indian subcontinent in response to changes in anthropogenic forcings, we have analysed the simulated daily data for selected climatic variables for the monsoon season during each of the 30-year period corresponding to 2050s. Figure 11 shows the temporal variations of simulated daily total rainfall averaged over central India from 1 May to 30 October for each of the 30 years along with daily mean for the 30-year period (thick line) for each of the four SRES 'Marker' scenarios. A comparison of Figure

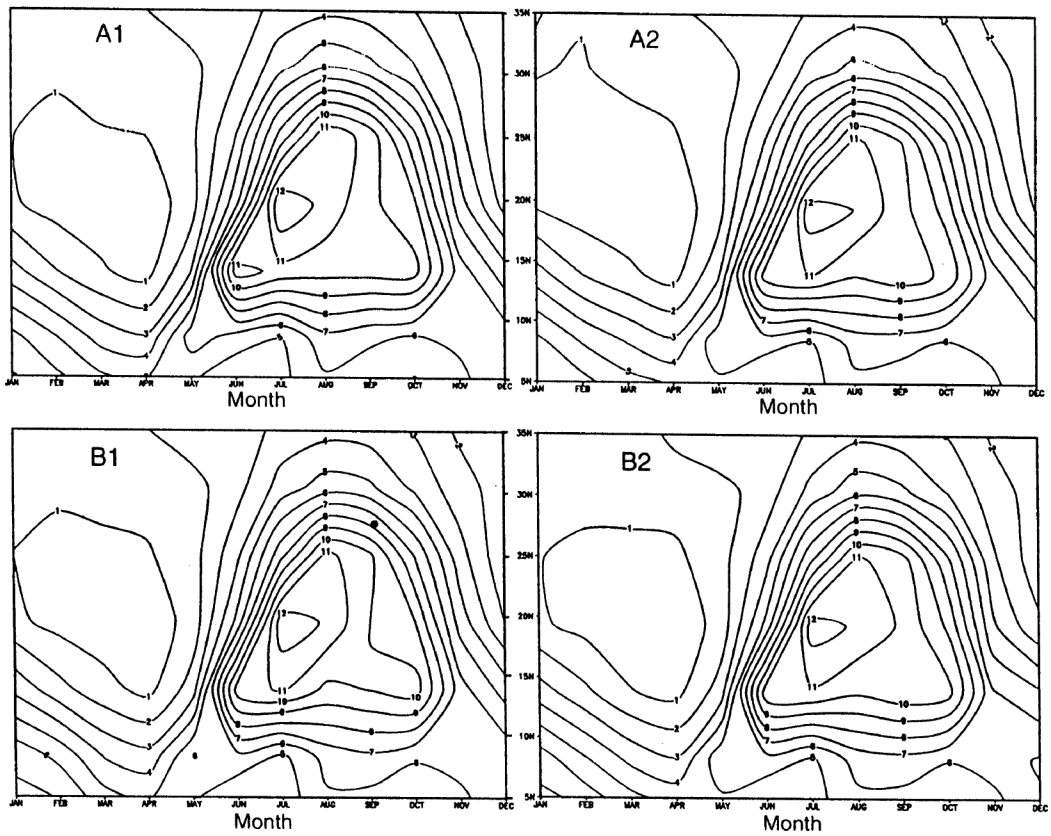

Figure 12. Temporal variation of model-simulated monthly zonal mean rainfall (mm/day) over Indian subcontinent (averaged over 65°E as simulated by the model for the four SRES 'Marker' forcing scenarios during 2050s.

11 with Figure 5 reveals many aspects of plausible changes in Indian summer monsoon activity over the central plains of India. The standard deviation of future projections of area-averaged monsoon rainfall centred around 2050s is not significantly different in each of the four scenarios relative to that simulated for the present-day atmosphere. This implies that the year-to-year variability in rainfall in central India during the monsoon season is not likely to change significantly in the future. More intense rainfall spells are, however, simulated by the model over the land regions under all the four scenarios (relative to that simulated for the present-day atmosphere), thus increasing the probability of extreme rainfall events in a warmer atmosphere (Figure 11).

It is interesting to note here that there are no appreciable shifts in rainfall maxima during July–August (still located at about 20°N) in the temporal variation of simulated monthly mean precipitation over the region in any of the four 'Marker' scenarios (Figure 12). The northward advancement of monsoon rains over India with the progression of the season, therefore seems quite robust. A detailed analysis of the daily rainfall data suggests that, under A1 and A2 scenarios, while the model still simulates the first spell of intense rainfall appearing over the southernmost part of India (5°N to 10°N) during the first week of June on an average, the spread of simulated onset date at 10°N (based on the criterion that rainfall at all grid points along 10°N in the region is 3 mm day^{-1} or more for at least three consecutive days) extends from 24 May to 11 June during the 30-year period centred around 2050s against between 29 May and 8 June of the present-day atmosphere. This implies the possibility of enhanced variability in the date of onset of summer monsoon over central India in a warmer atmosphere.

In order to ascertain the dominant time scales of monsoon circulation in the model and to examine the likelihood of changes in frequency of monsoon depressions in a warmer atmosphere which could contribute to enhanced precipitation over the Indo-Gangetic plains, spectral energy computations were performed on the detrended time series of simulated daily rainfall for each of the 30 consecutive years of the four SRES forcing simulations. For central India, the simulated daily rainfall exhibits statistically significant spectral peaks at periodicities not substantially different from those in control experiment. This suggests that no appreciable changes are likely in the number of monsoon depressions moving across the central plains of India in a warmer atmosphere.

Conclusions

The CCSR/NIES A–O GCM has limited skill in simulating the seasonal cycle as well as broad-scale features of the monsoon climatology over the Indian subcontinent. While the seasonality in rainfall over the region is realistically simulated, the area-averaged total monsoon rainfall is marginally higher than the observed rainfall. The daily rainfall intensity is only about two-thirds of the observed precipitation intensity over central India. There are no major deviations in the simulated rainfall maxima relative to observed patterns during the summer monsoon season. The model, however, does not realistically simulate the orographic rainfall pattern near the Himalayan foothills and along the Western Ghats.

The transient experiments with the CCSR/NIES A–O GCM under the four SRES 'Marker' scenarios suggest that annual mean area-averaged surface warming should range between 3.5 and 5.5°C over the region by 2080s. This warming would be more pronounced in winter than during monsoon season. During winter, India may experience between 5 and 25% decline in rainfall. The decline in winter-time rainfall over India is likely to be significant and may lead to droughts during the dry summer months. Only 10 to 15% increase in area-averaged monsoon rainfall is projected over the Indian subcontinent. The date of onset of summer monsoon over central India could become more variable in future. More intense rainfall spells are also projected in a warmer atmosphere, increasing the probability of extreme rainfall events.

There are several levels of uncertainty in the generation of regional climate change information. The first level is associated with emission scenarios of greenhouse gases and aerosols, that is strongly related to socio-economics of the countries in the region and could be strongly dependent on development pathways followed by individual nations. The conversion of emissions of greenhouse gases and aerosols into resulting concentrations with which global climate models are forced, introduces additional uncertainty. The second level of uncertainty is related to the simulation of the transient climate response by coupled A–O GCMs for a given emission scenario.

On the modelling aspects, uncertainties are associated with imperfect knowledge and/or representation of physical processes, limitations due to the numerical approximation of the model's equations, simplifications and assumptions in the models and/or approaches, internal model variability and inter-model or inter-method differences in the simulation of climate response to given forcing. The minimum scale at which climate change information can be reliable, which is determined by the model resolution, is still of the order of several hundred kilometres. By definition, coupled A–O GCMs cannot provide direct information at scales smaller than their resolution; neither can they capture the effect of forcing acting at sub-grid scales. Second, past analyses have indicated that even at their smallest resolvable scales, which still fall under our definition of regional scale, coupled A–O GCMs have substantial problems in reproducing present-day climate characteristics. It is also important to point out that regional climate observations are also sometimes charac-

terized by a high level of uncertainty, especially in regions characterized by complex topographical features.

Finally, the natural variability of the climate system adds a further level of uncertainty in the evaluation of a climate change simulation. In view of these constraints, the climate change scenarios presented here should not be viewed as a prediction, but only as a plausible projection for broader-scale impact assessments. In order to increase our skill in simulating the monsoon rainfall and its intra-seasonal variability over the Indian subcontinent, it is of foremost importance that we improve our understanding on the basic differences in parameterization techniques of physical processes adopted in the A–O GCMs and their effects on the simulation of regional precipitation. The model's sensitivity to the treatment of interaction between monsoon clouds and radiative processes appears to be a key factor.

1. Intergovernmental Panel on Climate Change, WMO–UNEP Report (eds Houghton, J. T. *et al.*), Cambridge University Press, UK, 1996, p. 572.
2. Senior, C. A. and Mitchell, J. F. B., *J. Climate*, 1993, **6**, 393–418.
3. Meehl, G. A. and Washington, W. M., *Climate Dyn.*, 1995, **11**, 399–411.
4. Latif, M. *et al.*, *J. Geophys. Res.*, 1998, **103**, 14375–14394.
5. Webster, P. J., Magana, V. O., Palmer, T. N., Shukla, J., Thomas, R. A., Yanai, M. and Yasunari, T., *J. Geophys. Res.*, 1998, **103**, 14451–14510.
6. Cess, R. D. *et al.*, *Science*, 1993, **262**, 1252–1255.
7. Gates, W. L., Cubasch, U., Meehl, G. A., Mitchell, J. F. B. and Stouffer, J., Report, WCRP-82, WMO/TD No. 574, World Meteorological Organization, Geneva, 1993.
8. Lal, M., Meehl, G. A. and Julie M. Arblaster, *Reg. Environ. Change*, 2000, **1**, 163–179.
9. Nakicenovic, N. *et al.*, Emissions Scenarios, A Special Report of Working Group III of the Intergovernmental Panel on Climate Change, Cambridge University Press, Cambridge, UK, 2000, p. 599.
10. Intergovernmental Panel for Climate Change, Assessment Report of IPCC Working Group I (eds Houghton, J. T. *et al.*) and WMO/UNEP, Cambridge University Press, Cambridge, UK, 2001, p. 881.
11. Lal, M., Cubasch, U., Voss, R. and Waszkewitz, J., *Curr. Sci.*, 1995, **69**, 752–763.
12. Numaguti, A., Takahashi, M., Nakajima, T. and Sumi, A., Report of a New Program for Creative Basic Research Studies (ed. Matsuno, T.), 1995, vol. 1–3, pp. 1–23.
13. Nakajima, T., Tsukamoto, M., Tsushima, Y., Numaguti, A. and Kimura, T., *Appl. Opt.*, 2000, **39**, 4869–4878.
14. Le Treut, H. and Z.-S. Li, *Climate Dyn.*, 1991, **5**, 175–187.
15. Louis, J., F., *Bound. Layer Meteorol.*, 1979, **17**, 187–202.
16. McFarlane, N. A., *J. Atmos. Sci.*, 1987, **44**, 1775–1800.
17. Takemura, T., Okamoto, H., Maruyama, Y., Numaguti, A., Higurashi, A. and Nakajima, T., *J. Geophys. Res.*, 2000, **105**, 17853–17873.
18. Yamanaka, Y. and Tajika, E., IAMAP Abstract No. M3–45, Yokohama, Japan, July 1995.
19. Suginohara, N. and Aoki, S., *J. Mar. Res.*, 1991, **49**, 295–320.
20. Semtner, A. J., *J. Phys. Oceanogr.*, 1976, **6**, 379–389.
21. Miller, J. R., Russel, G. L. and Caliri, G., *J. Climate*, 1994, **7**, 914–928.
22. Abe-Ouchi, A., Internal Report of Center for Climate System Research, 1997, vol. 2, pp. 117–130.
23. Emori, S., Nozawa, T., Abe-Ouchi, A., Numaguti, A., Kimoto, M. and Nakajima, T., *J. Meteorol. Soc. Jpn*, 1999, **77**, 1299–1307.
24. Kalnay, E. *et al.*, *Bull. Am. Meteorol. Soc.*, 1996, **77**, 437–471.
25. Legates, D. R. and Willmott, C. J., *Int. J. Climatol.*, 1990, **10**, 111–127.
26. New, M., Hulme, M. and Jone, P. D., *J. Climate*, 1999, **12**, 829–856.
27. Wigley, T. M. L. and Santer, B. D., *J. Geophys. Res.*, 1990, **95**, 851–865.
28. Meehl, G. A., *J. Climate*, 1994, **7**, 1033–1049.
29. Palmer, T. N., *Proc. Indian Nat. Sci. Acad.*, 1994, **A60**, 57–66.
30. Webster, P. J. and Yang, S., *Q. J. R. Meteorol. Soc.*, 1992, **118**, 877–926.
31. Sikka, D. R., *Proc. Indian Acad. Sci.* (*Earth Planet. Sci.*), 1980, **89**, 179–195.
32. Tropical Ocean Global Atmosphere, Monsoon Climate Research, Report of 2nd Session of the Monsoon Numerical Experimentation Group, WCRP-49, WMO-TD No. 392, 1990.
33. Krishnamurti, T. N. and Bhalme, H. N., *J. Atmos. Sci.*, 1996, **33**, 1937–1954.
34. Rao, Y. P., *Southwest Monsoon*, Meteorol. Monogr. No. 1, India Meteorological Department, New Delhi, 1976, p. 367.

ACKNOWLEDGEMENTS. We acknowledge the efforts of all those who supported the CCSR/NIES global climate model experiments. M.L. acknowledges the generous hospitality extended to him by the CCSR and NIES in Japan during the time this study was initiated. Part of the study was funded by the Indian Space Research Organization and Ministry of Environment and Forests.

Received 2 December 2000; revised accepted 3 October 2001